Identification of Key Active Species in the Conversion of C6 and C4 Sugars by Tungsten and Molybdenum Homogeneous Salts

Sabah El Mohammad, Noémie Noël, Olivier Proux, Antonio Aguilar Tapia, Jean-Louis F Hazemann, Christèle Legens, Céline Chizallet, Kim Larmier

Identification of Key Active Species in the Conversion of C6 and C4 Sugars by Tungsten and Molybdenum Homogenous Salts

Sabah El Mohammad,[a] Noémie Noël,[a] Olivier Proux,[b] Antonio Aguilar Tapia,[c] Jean-Louis Hazemann,[d] Christèle Legens,[a] Céline Chizallet[a] and Kim Larmier[a]*

[a] IFP Energies nouvelles, Rond-Point de l'Echangeur de Solaize, BP3, 69360 Solaize, France

[b] OSUG, UAR 832 CNRS, Université Grenoble Alpes, 38041, Grenoble, France

[c] ICMG, UAR 2607 CNRS, Université Grenoble Alpes, 38041, Grenoble, France

[d] Institut Néel, CNRS, Université Grenoble Alpes, 25 Avenue des Martyrs, 38042, Grenoble, France

ABSTRACT

Acquiring knowledge on the mechanisms of sugar transformation in valuable products is a prerequisite for the optimization of related catalytic processes. In the present work, we study the conversion of glucose and two other related sugars, mannose and erythrose, catalyzed by homogeneous molybdate- and tungstate-based catalysts through a combination of kinetic experiments and *in situ* XANES experiments. The body of results affords shedding light onto the active species and mechanism of the main reactions observed, namely retro-aldol condensation, a key step to produce short-chain products from biomass-based sugars, and

epimerization. In particular, we highlight the very distinct behavior of tungstates and molybdates in terms of reactivity and active species. Tungstates catalyze epimerization and retro-aldol condensation through two different mononuclear bidentate species (respectively O1,O2 and O1,O3), likely of +VI oxidation state of tungsten. Molybdates promote epimerization through a binuclear, tri- or tetradentate species (at least O1,O2,O3) and retro-aldol condensation by a mononuclear bidentate species (O1,O3).

KEYWORDS

Biomass, Carbohydrate, Catalysis, Kinetics, XAS, Tungstates, Molybdates

TOC GRAPHICS

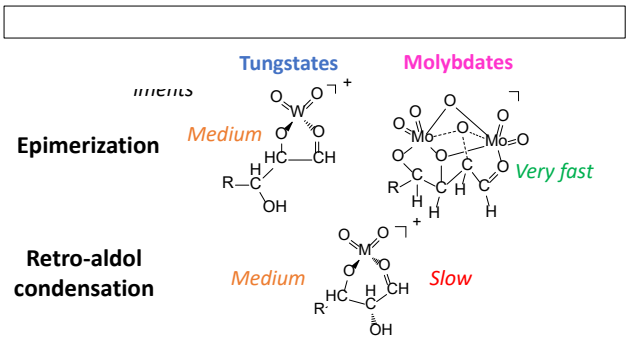

1. Introduction

The conversion of glucose and other biomass-based sugars to valuable products has been considered since decades as an exciting research topic.[1,2] One of the most important transformations is the conversion of glucose to ethylene glycol (EG) by a so-called "hydrogenolysis" of sugars.[3–6] The process occurs mainly through a cascade reaction involving the C-C bond cleavage of glucose by retro-aldol condensation reaction (RAC) into C_2 intermediate (glycolaldehyde - GA), followed by the hydrogenation of this intermediate to the

desired product (***Figure 1***).[7] In a first step glucose is cleaved to form one molecule of GA and erythrose. The latter is a C_4 sugar that in turn undergoes retro-aldol condensation to form two additional GA molecules. The reaction network involves many side reactions. In particular, epimerization of glucose into mannose takes place. Isomerization of glucose gives rise to fructose that by undergoing C-C bond cleavage produces C_3 intermediates (glyceraldehyde and dihydroxyacetone), yielding C_3 polyols (1,2-propanediol) upon hydrogenation, thus lowering the EG yield. Additionally, polymeric degradation products called 'humins' are formed in parallel, that are not detected by conventional analytic methods (like High Performance Liquid Chromatography, HPLC), leading to loss in carbon balance. Therefore, the choice of a selective catalyst for a direct retro-aldol condensation constitutes the key element for the success of the process.

The ability of heterogenous and homogenous tungsten-based catalysts in association with a hydrogenation catalyst to convert cellulose and cellulose-derived glucose for the production of short chain polyols such as ethylene glycol (EG) was intensively demonstrated by Zhang and co-workers.[8–12] High yields (76%) of ethylene glycol are reached, showing the high efficiency of tungstate salts to catalyze selectively the retro-aldol condensation over isomerization reaction. Conversely, Bilik and co-workers have investigated the production of rare sugars over homogenous molybdate salts in an acidic medium and shown for instance that mannose could be efficiently produced from glucose by epimerization,[13–16] while a similar reaction carried out with W-based salts turns out much less efficient. Thus, tungstate and molybdate ions in aqueous solutions, that lead to very different selectivity despite a number of similarities regarding their speciation,[17,18] are a very interesting family of species for the development of sugar conversion catalysts.

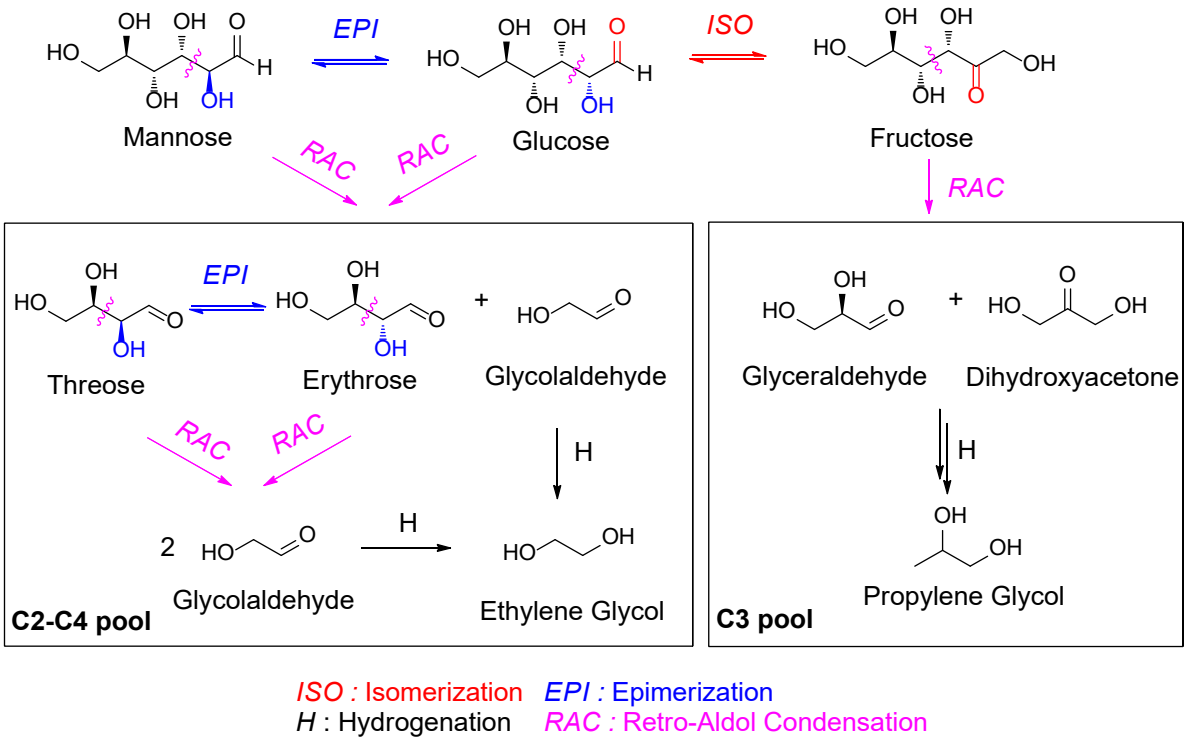

Figure 1. *Reaction routes possibly involved in glucose, mannose and erythrose conversion over tungstate and molybdate oxyanions.*

Although these reactions were investigated in the literature, there still lacks a fundamental understanding of this reactivity at a molecular scale regarding the nature of the active species, in terms of the oxidation state of the metal or interaction between the substrate and active species (nuclearity, structure of complex…).

Regarding the epimerization of sugars catalyzed by homogeneous molybdate species, Bilik and coworkers have conducted a variety of seminal work and proven that the active species are binuclear species of molybdates forming a complex with a linear hydrate form of the substrate sugar.[19,20] This was supported by more recent DFT studies, that also support the fact that isostructural complexes involving tungstates are less reactive.[21] Much less clear evidence exists concerning the RAC reaction. Zhang et al. proposed the involvement of a "tungsten bronze species" featuring partially reduced W centers H_xWO_3, formed from WO_3 heterogeneous

species, although no clear structure is proposed for the active site.[10,22] The idea of the involvement of a reduced species is also supported experimentally in the case of heterogeneous WO_3 species in the presence of Cu particles[23] and by recent DFT calculations for homogeneous species.[24] However, kinetic studies carried out with homogeneous tungstate species have shown that the RAC reaction occurs even in the absence of a hydrogenating catalytic function at noticeable rates,[25] which questions the involvement of reduced species. As for the active species, Liu et al. have shown by kinetic experiments including the use of deoxy-glucose as substrates that in the case of the conversion of glucose with WO_3 as a catalyst, the presence of both α- and β- hydroxyl groups with respect to the carbonyl function of glucose are required, and thus propose a tridentate coordination mode of glucose as an active species.[26] In the case of homogeneous species, Zhang et al. proposed from kinetic experiments, in particular from the reaction rate orders for the sugar and tungstate species, the intermediacy of putative mononuclear tungstate species complexing three to four sugar molecules.[27] However, such species were not observed in previous work addressing the speciation in aqueous solutions of sugar and tungstate or molybdate ions.[28–33] What is more, these works show that homogeneous tungstate and molybdate ions share similarities in their speciation with sugars, in particular the dependence on the pH of the solution. So far, no relationship could be made between this speciation and the reactivity for either metal species.

In the present work, we address the reactivity of sugars catalyzed by homogeneous tungstate or molybdate based species and question the relationship with the complexes observed in our previous contributions.[28,29] A kinetic study is carried out by taking into consideration the complexity of the reaction medium from both point of views, the metal, and the sugar. As for the metals, tungstate and molybdate oxyanions are known to have pH and concentration dependent behavior in aqueous solution.[17,18] The variation of their aqueous speciation as function of reaction conditions (metal concentration, pH, temperature) is taken into

consideration. Furthermore, an *in-situ* follow-up of the reaction is conducted using X-ray absorption near edge spectroscopy (XANES) to extract information about the environment and oxidation state of the metal, which are considered as critical parameters in catalysis. We also conducted a set of experiments to gain additional information on the reaction mechanism, including suppression of some of the functional groups of the sugar using deoxy glucose products at the different carbon positions. This approach leads us to the elucidation of the structure of the key intermediates promoted by molybdates and tungstates for glucose, mannose and erythrose in epimerization and retro-aldol condensation.

2. Methods

Catalytic tests

The catalytic activity of several tungsten and molybdenum precursors (Sodium molybdate dihydrate ($Na_2MoO_4 \cdot 2H_2O$), ammonium heptamolybdate tetrahydrate [$(NH_4)_6Mo_7O_{24} \cdot 4H_2O$] (AHM), Sodium tungstate dihydrate ($Na_2WO_4 \cdot 2H_2O$) and ammonium metatungstate [$(NH_4)_6H_2W_{12}O_{40}$] (AMT)), was quantified with D-glucose, D-mannose, D-erythrose and glycolaldehyde at various sets of conditions (temperature, pH, concentration of the metal and the atmosphere). Sugars and catalysts are used as received (Sigma Aldrich). In the following, for the sake of clarity, we omit the absolute stereochemical information of the sugars and simply refer to glucose, mannose, erythrose etc.

Conversion of sugars was carried out in batch mode in a stainless-steel reactor equipped with an injection chamber. In a typical batch experiment, the reactor was loaded with 50 mL of an aqueous solution containing the catalyst, of which the pH was adjusted to the target value. After flushing 3 times with nitrogen gas, simultaneously while agitating with a magnetic stirrer, the reactor was hermetically closed and pressurized at a pressure of 3 bar and heated to the desired temperature. The feeding tank was loaded with 10 mL of an aqueous sugar solution of

the appropriate concentration, flushed 3 times, and then charged with pure H_2 or N_2 gas at 40 bar. Once the desired temperature was reached, the solution of sugar is poured into the reactor in a short amount of time (few seconds). The reactor was then pressurized at 40 bar and the reaction started by an agitation at 1100 rpm. Samples were manually taken from the reactor at a certain time interval for analysis.

In a standard experiment, 5.0 mmol L^{-1} of the sugar was converted at 150 °C, over tungsten and molybdenum-based homogenous catalysts at 1.3 mmol L^{-1} of metals concentration. Different pH ranges are considered since the current parameter was found to be governing metal and metal-sugar speciation in aqueous solution.[28,29] The pH was measured at room temperature in a separate experiment reproducing the same conditions of concentrations and volumes in the reactor and injection chamber by a conventional glass electrode apparatus. The pH value was adjusted to the desired value by addition of a few drops of NaOH solutions (3 mol.L^{-1}) or HCl (1 mol L^{-1}) to the initial content of the reactor. The concentration of metals varied from 1.3 mmol L^{-1} to 0.1 mmol L^{-1} while the concentration of the sugar was kept constant at 5.0 mmol L^{-1} in all experiments. The experiments were done at a temperature ranging from 150 to 180 °C.

The involvement of each hydroxyl group was examined by employing deoxygenated versions of glucose. 2-deoxy-D-glucose (purchased from Fisher Scientific), 3-deoxy-D-glucose, 4-deoxy-D-glucose, and 6-deoxy-D-glucose (purchased from Santa Cruz Biotechnology laboratories) (***Figure S1*** in Supporting Information) were converted at 180°C (to ensure a high activity of the metal in the RAC reaction) at metal and reactant concentrations of respectively 1.3 mmol L^{-1} and 5.0 mmol L^{-1} under 40 bar of N_2.

The effluents of the reaction were analyzed by high performance liquid chromatography (HPLC). The separation line is equipped with a REZEX RCM-Monosaccharide Ca^{2+} (8%) column (Phenomenex). The apparatus is equipped with a differential refractometer to detect the

separated products. Pure water flows as a mobile phase at a rate of 0.6 mL min^{-1}. The injected volume of the sample is 20 µL and the temperature inside the column and the detector were respectively 90 and 50 °C. Typical chromatographs are shown on ***Figure S2.*** The identification of the products was made by comparing the HPLC chromatograms of sugar transformation to the HPLC chromatograms of standard chemicals. The concentrations of the products in each sample were quantified by means of the response factor associated with each chemical species for which the values are given in ***Table S1***. This method allows for separating and quantifying unambiguously glucose, mannose, glycolaldehyde, dihydroxyacetone, erythrose and 5-HMF. We note here that threose and fructose are co-eluted, hence the identification and quantification of fructose was carried out by considering that quantity of threose is negligible (unless the reaction is carried out with erythrose as a substrate, in which case the corresponding signal is assigned to threose). The maximum yield y_{max} of RAC and epimerization or isomerization products and the carbon balance (CB) throughout the reaction time are calculated according to equations (1) and (2).

$$y_{max} = \frac{\max [A_i]}{[A_i]_{th}} \quad (1)$$

$$CB(t) = \frac{\sum n_{C,i}[A_i](t)}{\sum n_{C,i}[A_i](0)} \quad (2)$$

where $[A_i]$ is the concentration of a given compound A_i, $[A_i]_{th}$ the theoretical maximum amount of species A_i affordable from the reactants, and $n_{C,i}$ the number of carbon atom of compound A_i.

Uncertainties, when given, are estimated based on the repetition of a catalytic test up to three times.

In situ X-ray Absorption Near Edge Structure (XANES) experiments

In-situ experiments were conducted at the European Synchrotron Radiation Facility (ESRF, Grenoble, France) at the CRG-FAME BM30 beamline,[34,35] in a high pressure/high temperature cell (HP vessel) designed for X-Ray Absorption Spectroscopy (XAS) in which pressure and temperature are controlled independently up to respectively 1200 °C and 2000 bar for aqueous solutions (***Figure S3***).[36] The vessel is designed with three windows, two of them on the beam axis allowing the entry and the collection of transmission absorption spectra. The last one is devoted for acquiring fluorescence photons. The aqueous samples were placed inside the internal cell made of glassy carbon. The cylindrical carbon tube was enclosed from both sides with a pair of bellows transferring the pressure to the sample. The conversion of glucose, mannose and erythrose over tungstate and molybdate catalysts was conducted at the different reaction conditions mentioned above in the experimental section of the catalytic tests.

Storage ring was operated at 200 mA with refill every hour. Spectra were recorded in transmission mode using Si diodes collecting photons scattered by a kapton foil to measure the incident and transmitted photons intensities. Energy of the monochromatic beam was tuned using a Si(220) liquid-nitrogen cooled double-crystal monochromator surrounded by two Rh-covered mirrors for harmonics rejection.[34] Second crystal of the monochromator was dynamically bent in order to focus the beam on the horizontal direction. First mirror curvature was adjusted in order to collimate the beam on the vertical direction, and so to optimize the energy resolution and the photons flux on the sample, while second mirror was bent in order to focus the beam on the vertical direction. Thanks to these elements, the beam spot on the sample was 200 × 100 µm² (HxV, full width half maximum values). Energy calibration was ensured for each scan by measuring the XAS signal of either W or Mo metallic foil in double transmission, simultaneously to the studied solutions, with reference energies set at

10207 eV and 20000 eV respectively. All processing of the spectra was carried out using the Demeter software suite.[37]

3. Results and discussion

3.1. Sugars conversion over tungstate and molybdate oxyanions: an overview

Figure S2a,b illustrates the chromatograms of glucose transformation catalyzed by ammonium metatungstate (AMT) and ammonium heptamolybdate (AHM) respectively at 15 min of reaction time. In both chromatograms one can observe the co-existence of several types of reaction products. In the following, we report mainly a quantification of the RAC main product, glycolaldehyde (GA) and the products of side reactions (epimerization and isomerization).

Blank experiments were carried out for the conversion of glucose at 150 °C and 180 °C (***Figure S4a,b*** in the Supporting Information) under N_2. Only very low yields of GA are obtained (1 and 3% of GA yield at 150 and 180 °C, respectively, at 105 min of reaction time), indicating that a catalyst is essential to promote retro-aldol condensation. However, significant glucose degradation into unknown products (humins) is observed even without a catalyst. Additionally, to assess the effect of basic solutions on the catalysis, two experiments were conducted at two different pH values 10 and 12 with NaOH concentrations of 0.5 and 0.8 mmol L^{-1} respectively (***Figure S4c, d***). Under the catalysis of sodium hydroxide, glucose afforded mainly fructose (y_{max} = 11% and 23% at pH 10 and 12 respectively), in line with previous literature.[38] Dihydroxyacetone and glycolaldehyde, products of fructose and glucose cleavage respectively are obtained in low yields (at pH 10.5: 1.8% and 0.6% of GA and DHA respectively, at pH 11.8: 3.6% and 3.4 % of GA and DHA respectively). Therefore, acido-basic catalysis may promote to some extent retro-aldol condensation, which is discussed below.

The formation and consumption of the various products for the conversion of different aldoses (glucose, mannose and erythrose) over AMT and AHM catalysts are shown on ***Figure 2***.

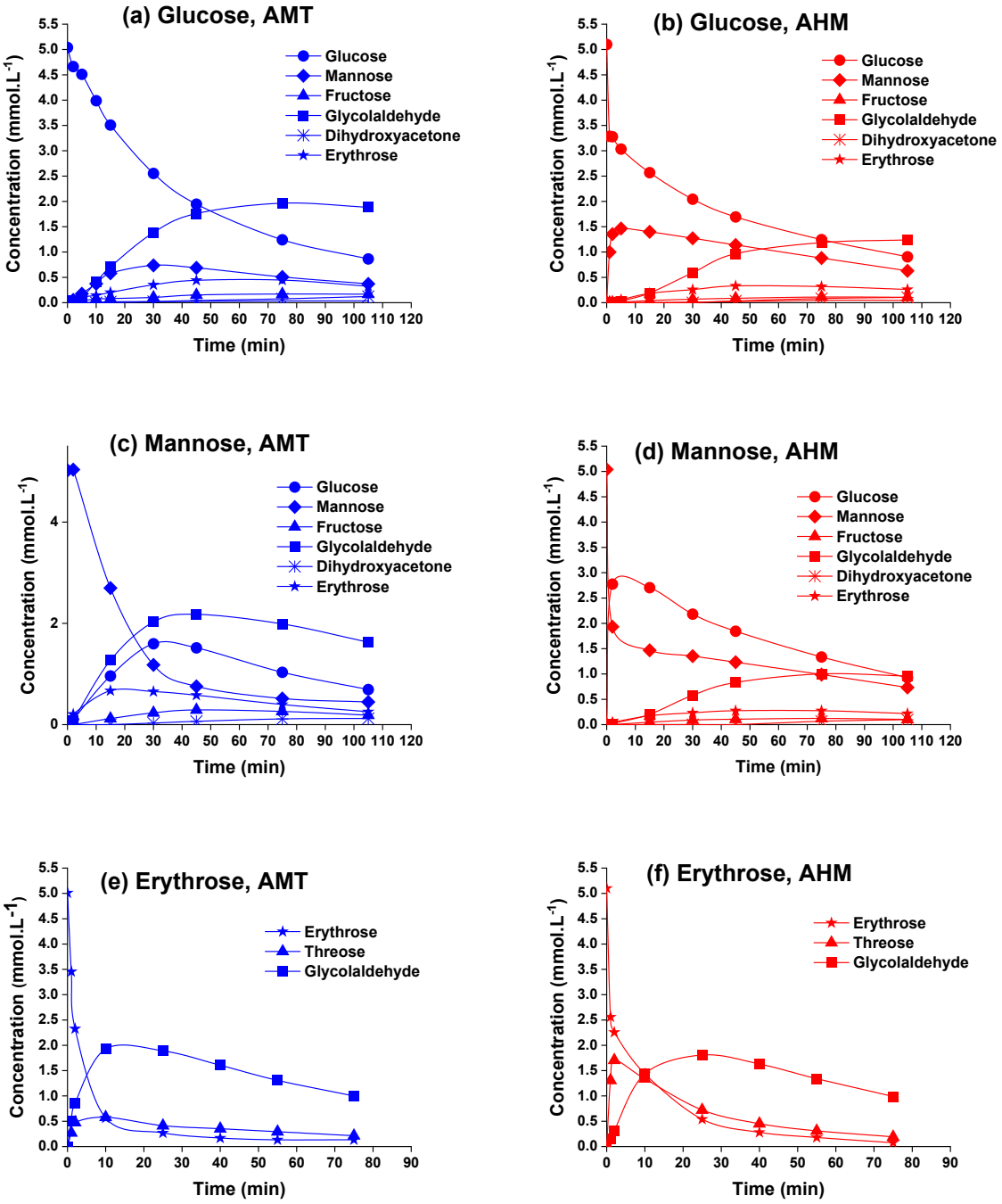

Figure 2. *Evolution of the concentration of aldoses and their conversion products over AMT (pH 5) and AHM (pH 4) catalysts at 150 °C under 40 bar of N_2 pressure as function of reaction time, sugar, and metal concentrations of respectively 5.0 and 1.3 mmol L^{-1}.*

As a general observation with both catalysts, mainly products of retro-aldol condensation (GA, erythrose) and epimerization are obtained. The catalytic activity of both metals for the different transformations are evaluated by the estimation of the initial reaction rates. The initial rate of retro-aldol condensation and epimerization are evaluated as the initial formation rate of GA and the corresponding epimer respectively obtained by fitting the experimental data with linear trend curves and measuring their slope. The initial formation rates of these different products at different reaction conditions for the three aldoses are given in ***Table 1***. Fructose (the isomer of glucose and mannose) and dihydroxyacetone (product of fructose retro-aldol condensation) are formed in extremely low quantities with both metals (cumulated maximum yields of 3.4% with AMT and 2.2% with AHM), and thus are minor products of the reaction in comparison of the two main paths EPI and RAC.

Table 1. *Formation rates of GA and epimers of sugars with tungsten and molybdenum-based catalysts. r_f: initial formation rate (mmol L^{-1} min^{-1}), t_1: time at which the maximum amount the product is reached (min), and y_{max}: the corresponding maximum yield percentage, see equation (1). These results are obtained from sugars conversion at 150 °C, under 40 bar of N_2 at sugars and metals concentrations of respectively 5.0 and 1.3 mmol L^{-1}.*

	Glucose			**Mannose**			**Erythrose**		
Retro-Aldol Condensation (RAC)									
Catalyst	r_f (±9%)	t_1	y_{max}(±5%)	r_f (±9%)	t_1	y_{max}(±5%)	r_f (±9%)	t_1	y_{max}(±5%)
AMT (pH 5)	0.048	75	13.1	0.086	45	14.5	0.430	10	19.2
AHM (pH 4)	0.026	120	8.3	0.019	75	6.7	0.156	25	18.0
Na_2WO_4 (pH 7)	0.073	45	12.9	0.124	30	14.7	nd	nd	nd
Na_2MoO_4 (pH 6)	0.023	75	4.1	0.025	105	5.3	nd	nd	nd
AMT + NaOH (pH 11)	0.094	45	13.5	0.123	30	14.6	0.551	10	18.3
AHM + NaOH (pH 10)	0.015	45	4.4	0.020	65	4.9	0.284	2	5.6
Epimerization (EPI)									
Catalyst	r_f (±8%)	t_1	y_{max}(±6%)	r_f (±8)	t_1	y_{max}(±6%)	r_f (±8)	t_1	y_{max}(±6%)
AMT (pH 5)	0.041	30	14.6	0.065	30	31.8	0.237	10	11.6
AHM (pH 4)	0.678	5	29.2	1.387	2	55.4	0.853	2	34.0
Na_2WO_4 (pH 7)	0.029	30	10.2	0.035	30	17.2	nd	nd	nd
Na_2MoO_4 (pH 6)	0.016	75	12.0	0.032	75	26	nd	nd	nd
AMT + NaOH (pH 11)	0.024	30	8.2	0.029	30	17.0	0.110	5	6.6
AHM + NaOH (pH 10)	0.005	75	6.6	0.020	65	24.8	0.027	5	1.1

Over AMT catalyst, glucose is converted to GA and mannose (**Figure 2a**) with similar initial reaction rates, affording almost equal yields of products at short reaction times (15 min). The maximum amount of GA is obtained at 75 min while mannose reaches a maximum concentration at 30 min of reaction time. When mannose is converted over AMT (**Figure 2c**), GA is formed with slightly higher initial reaction rate than glucose as product of epimerization. As for erythrose as a reactant (**Figure 2e**), the maximum yield of GA and threose (the epimer) are almost similarly obtained at 10 min of reaction time. However, the initial formation rate of GA is twice higher than the formation rate of threose. According to these results one can say that tungsten is active for both transformations (RAC and epimerization).

The conversion of the three sugars over AHM at pH 4 to GA always occurs with lower initial reaction rates than the conversion to the epimer (**Table 1**). Consistently, the epimers are obtained in higher yield than GA at shorter reaction time. These results indicate that molybdenum is more selective for the epimerization of sugars than for retro-aldol condensation. Molybdenum catalyzed epimerization of the three sugars always occurs at higher reaction rates than with tungsten and reaches higher yields at shorter reaction times. According to **Table 1**, higher initial formation rates of GA are recorded for tungstate catalyst with the three sugars compared to molybdate. Conversion of erythrose to GA is faster compared to the C_6 sugars with both catalysts, with formation rates for GA larger by about one order of magnitude (0.430 vs. 0.048 and 0.086 for glucose and mannose, respectively, over AMT; 0.156 vs. 0.026 and 0.021 for glucose and mannose respectively over AHM). The difference in formation rates of GA from glucose (0.048 mmol L^{-1} min^{-1}) and mannose (0.086 mmol L^{-1} min^{-1}) is much smaller. This shows that erythrose is much more prone to undergo C-C bond cleavage than the C_6 aldose, which is qualitatively in line with our previous results, which showed conversion of erythrose

into various products including GA even at room temperature over a couple of hours, while mannose and glucose remained unconverted in the same conditions.[29]

The concentration of GA increases as the reaction begins due to the conversion of glucose, mannose and erythrose by RAC then after reaching a certain maximum, the concentration starts to decrease, indicating that GA undergoes further side transformations (condensation or degradation). To get more quantitative information on this phenomenon, we compare in **Figure 3** the evolution of the carbon balance in experiments using glucose, erythrose or glycolaldehyde as substrate at different reaction conditions.

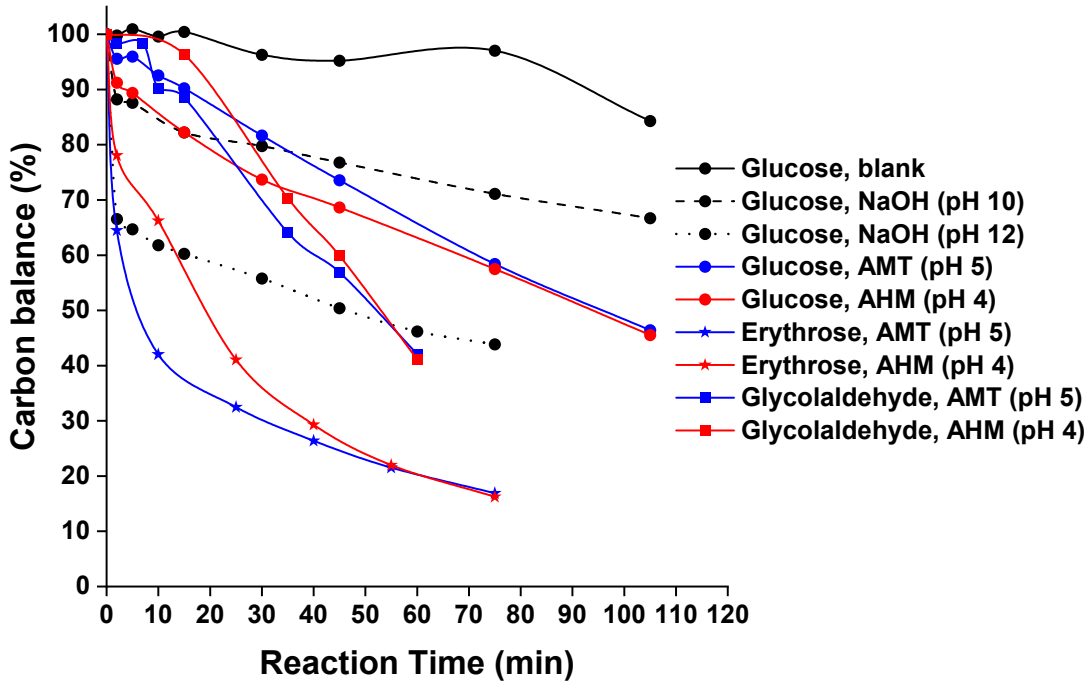

Figure 3. *Carbon balance calculated according to Equation (2) evolution as a function of reaction time for the conversion of different feedstocks at different reaction conditions. The conversion was carried at 150 °C under 40 bar of N_2. Initial glucose and erythrose concentrations of 5.0 mmol L^{-1}, Initial glycolaldehyde concentration of 10.0 mmol L^{-1} and metal concentration of 1.3 mmol L^{-1}.*

The carbon balance of the reaction decreases over time, which is explained by the formation of polymeric compounds (humins)[39] and other side products that cannot be identified using the separation techniques used herein. A non-negligible quantity of organic acids, especially at long

reaction times, is also formed among the degradation products (as visible on the chromatograms), however, no effort was done to precisely qualify and quantify them. In the case of glucose, the carbon loss is significantly less important in the absence of a catalyst (about 15% at the end of the reaction, related to the hydrothermal decomposition of the sugar) than in the presence of either AHM or AMT, for which it is similar and about 50% at 110 min of reaction time. This clearly shows that the catalysts play a role in the degradation reactions, either by catalyzing side transformations of sugars themselves, or that of the products of the reaction (such as GA). The carbon loss for GA conversion trends similarly with both metals and it is similar to the degradation of glucose until 35 min of reaction time while after 60 min the degradation is more pronounced for GA reaching around 60%. However, these results do not show a particularly faster degradation of GA compared to that of glucose. Interestingly, erythrose degradation was the fastest, as the carbon loss attained almost 80% after 75 min of reaction time. Tungsten catalyzes faster the degradation of erythrose than molybdenum (carbon loss at 25 min of 60% with W vs. 25% with Mo). This points toward erythrose as the main intermediate of degradation in the reaction scheme, which was not reported in the past literature that rather incriminated glycolaldehyde[10,25] as a key intermediate for degradation

In the following, and according to the observations reported above, we reason under the following hypotheses and simplifications from ***Figure 1***:

- Epimerization and retro-aldolisation of each sugars are parallel reactions;
- Isomerization of glucose to fructose and associated secondary reactions are neglected, unless otherwise noted;
- Degradation reactions (*ie* formation of humins) may occur from each compound (glucose, mannose, erythrose or glycolaldehyde).
- We essentially reason about the initial rates of formation of the products (epimer and glycolaldehyde, when starting from glucose) measured within the 10 first minutes of the

reaction, so we can approximate that the influence of secondary reactions remains negligible.

3.2. Kinetic measurements

We then carried out a set of experiments aiming at gaining several kinetic parameters for this reaction. Given that the active species is not known so far, and that molybdate and tungstate species have complex speciation in aqueous solutions, especially in the presence of sugars,[28,29,31–33] it is not possible to propose *a priori* an exact formalism for the rate equation. We thus chose to hypothesize a simplified formalism for each examined reaction (epimerization and RAC) including the concentration of the sugar and that of the total amount of metal as described in Equation (3).

$$r_f \approx k_{app}[Sugar]_0^a[M]_0^b \quad (3)$$

where r_f is the initial formation rate, k_{app} is the apparent rate constant, a the apparent order with respect to the sugar and b the apparent reaction order with respect to the metal, considering the total concentration of metal atoms $[M]_0$ (M = W or Mo), independently of the speciation. The apparent rate constant may be written under the formalism of Arrhenius as in Equation (4).

$$\mathrm{k_{app}} = A_{app}\exp\left(\frac{-\mathrm{E_{a,app}}}{\mathrm{RT}}\right) \quad (4)$$

where A_{app} is the apparent pre-exponential factor, R is the universal gas constant (8.314 J mol^{-1} K^{-1}), T is the temperature of the reaction (K), and $E_{a,app}$ is the apparent activation energy of the reaction (J mol^{-1}). We determine the values of the partial orders and apparent activation energies in the following sections for epimerization and RAC, firstly in the case of glucose conversion.

Order of the reaction with respect to the catalyst

To search for the order of the reaction with respect to the catalyst, experiments with the same initial glucose concentration but different initial metals concentrations were carried out.

Equation (3) may be derived as Equation (5):

$$\ln(r_f) = \ln\left(k_{app}[Sugar]_0^a\right) + \mathrm{b}\ln([\mathrm{M}]_0) \quad (5)$$

Considering that k_{app} depends only on the temperature, the term $\ln\left(k_{app}[Sugar]_0^a\right)$ is a constant. Thus, we can plot $\ln(r_f)$ as a function of $\ln([M]_0)$ of which b is the slope and stands for the partial order with respect to the Mo or W concentration. The corresponding order plot of RAC (formation of GA) and of epimerization from glucose are presented in **Figure 4.** The initial rate of the reaction increases as the concentration of the metals increases. Note that we plotted for a different reaction temperature for epimerization and RAC since the reaction was either too fast (EPI) or too slow for employing the same temperature for a fair determination of the reaction order. All the corresponding temporal evolution curves are given in **Figure S5.**

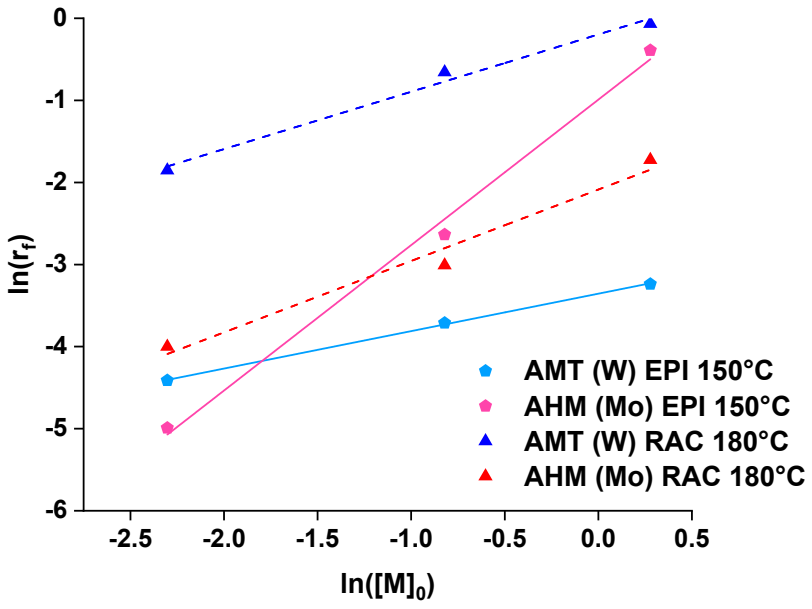

Figure 4. *Order plot with respect to the catalyst* ***concentration*** *in glucose conversion experiments, for the production of GA at 180 °C and for the production of mannose (epimer of glucose) calculated at 150 °C. Glucose concentration: 5.0 mmol L^{-1}. r_f is expressed in mol L^{-1} min^{-1}.*

Reasonable linear plots are obtained, see data in **Table S2**. For the RAC reaction, we measure similar apparent reaction order for W and Mo, with values of 0.70 ± 0.16 and 0.87 ± 0.28, respectively. The values are close to unity, which might suggest a mononuclear active species, however, given the uncertainty of our measurements, we may not draw further conclusion regarding the comparative reactivity of AMT (W) versus AHM (Mo). However, in the case of epimerization, we measure apparent reaction orders with respect of W and Mo of respectively 0.45 ± 0.02 and 1.77 ± 0.24. In this case, the difference is clearly significant, with the former being close to 1/2th order and the latter close to a second order reaction. The latter is consistent with the binuclear active species proposed by Bilik and others.[19,20] The significantly different value for W-based species suggests that either a different species is involved, or that the equilibria leading to the formation of the active species are significantly distinct for both metals (and thus the stability of the active species). Additionally, we note that epimerization has a partial order close to two with molybdenum, which is markedly distinct from the partial order of RAC, close to unity, which points to different active species for both reactions. The comparison in the case of tungstate is not that clear, though.

Apparent activation energy

Assuming that the conversion of glucose over AMT or AHM follows a first order with respect to glucose, as determined by Zhang et al. in the case of AMT,[10] combining Equations (3) and (4) yields Equation (6).

$$\frac{r_f}{[Gluc]_0} = A_{app}.\exp\left(\frac{-\mathrm{E_{a,app}}}{\mathrm{RT}}\right) \quad (6)$$

By applying the natural logarithm to Equation (6), the apparent activation energy of the reaction may be determined. We evaluated the conversion of glucose at different temperatures (see **Figure S6**). The corresponding Arrhenius plots are shown on **Figure 5**, and the details of the linear fittings are given in **Table 2.** The apparent activation energies are calculated from the

slopes of the linear fittings, and the pre-exponential factors A_{app} from the intercepts. Note that for the epimerization reaction, we chose a different temperature range (80-120 °C) in order to better measure the rates, as the reaction is very fast at higher temperatures.

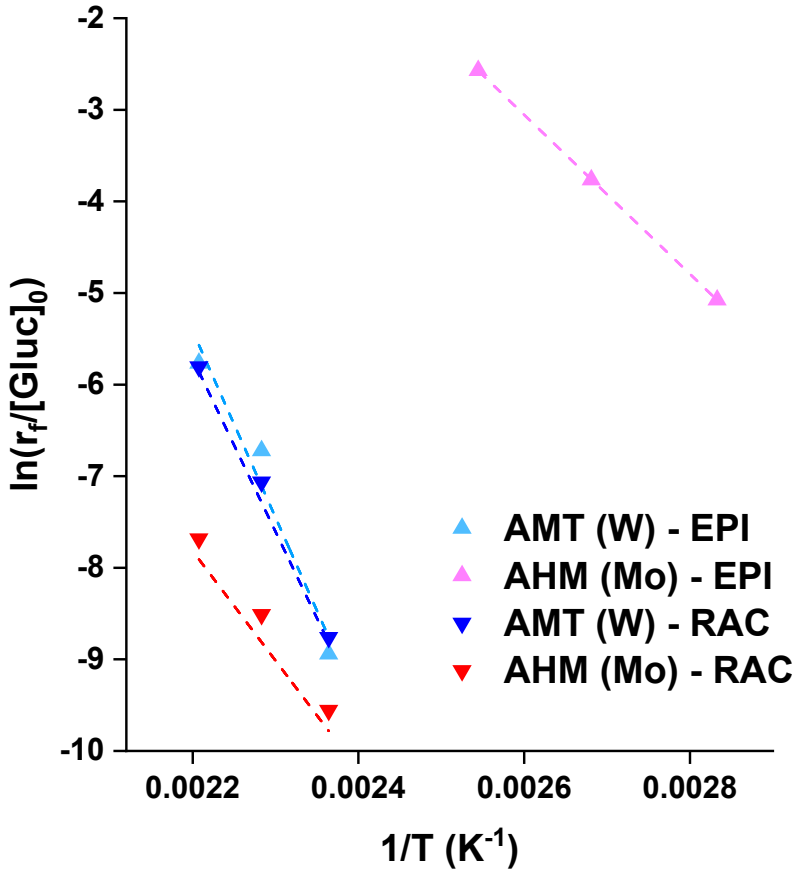

Figure 5. *Arrhenius plot for glucose retro-aldol condensation over tungstate and molybdate catalysts. $r_f/[Gluc]_0$ is expressed in min^{-1}.*

In the case of the RAC reaction, we find apparent activation energies 157 ± 10 kJ mol^{-1} for tungstate and of 99 ± 5 kJ mol^{-1} for molybdate catalysts. The value for tungsten-based catalyst is in line with that determined by Zhang and coworkers of 147 kJ mol^{-1}.[25] Surprisingly, although the production of GA displays lower reaction rates with molybdate-based catalyst, its apparent activation energy is lower than that with tungstates. The intercepts of the plots, which yield pre-exponential factors of 3.9 10^{15} s^{-1} and 1.3 10^{8} s^{-1} for tungstates and molybdates, clearly indicate that the difference in activity is driven by this parameter, that encompasses both entropic effects

as well as population of active species. Hence, we find that either of these factors drives the selectivity towards RAC rather than energetic parameters.

In the case of the epimerization reaction, the apparent activation energies calculated for tungstate and molybdate are of 169 ± 35 kJ mol^{-1} and 72 ± 1 kJ mol^{-1}, with pre-exponential factors of 1.3 10^{17} s^{-1} and 3.1 10^{8}, respectively. In this case, the rates of epimerization are driven by the energetics rather than by entropic and population factors. This opposes the observation made in the case of RAC, and this together points towards different active species and mechanisms.

Table 2. *Linear fitting details of the Arrhenius plots presented on* ***Figure 5****.*

Reaction	Metal	Precursor	$E_{a,app}$		$\ln(A_{app})$		R^2
			Value	Uncertainty	Value	Uncertainty	
RAC	W	AMT	157	10	36.0	2.8	0.996
	Mo	AHM	99	5	18.8	1.3	0.998
EPI	W	AMT	169	35	39.4	9.7	0.958
	Mo	AHM	72	1	19.5	1	0.999

Precursor and pH effect on the conversion of sugars

We now examine the effect of varying the metal speciation, either by changing the metal precursor or by varying the pH, the latter of which was found to be determinant for the speciation of metal/sugar solutions.[29] The pH of the reaction medium for the conversion of the different sugars was increased by the addition of a given amount of NaOH solution in the reactor with AMT and AHM. We alternatively employed sodium tungstate Na_2WO_4 and molybdate Na_2MoO_4 as alternative catalyst precursors, which spontaneously generate at the concentrations employed in this study aqueous solutions at pH of 7 and 6, respectively (vs. 5 and 4 for AMT and AHM). ***Table 1*** gathers the initial rates and maximum yields obtained in this series of experiments with glucose, mannose and erythrose as substrates, while ***Figure 6*** shows the evolution of the initial rates of RAC and EPI as a function of the starting pH. The corresponding concentration over time graphics are shown on ***Figure S7*** (RAC) and ***Figure S8*** (EPI). The

kinetics of RAC and EPI for the conversion of C_6 aldoses over Na_2WO_4 matches well the evolution of the kinetics for the conversion of these sugars over AMT catalysts conducted at pH 4 and 11 (***Figure 6***). Therefore, we consider that the activity of the metal is not impacted by the precursor type as much as it is impacted by the pH of the medium. This observation is in line with the results reported elsewhere in which we show that pH is a principal governing factor for the metal's aqueous speciation in addition to the concentration of the metal independently of the precursor type.[28,29]

Among the various effects that we observe upon increasing the pH, some may be assigned to the specific contribution of hydroxide ions (see dedicated experiments on ***Figure S4***):

- the initial rate of GA formation slightly increases for the conversion of the different sugars over both metals. The increase of GA initial formation rate could be assigned to the presence of hydroxide ions or to the change of tungstate speciation with changing pH. RAC initial rates for the production of GA as product of glucose retro-aldol condensation over hydroxide ions (***Figure S4***) are of 0.008 mmol L^{-1} min^{-1} at pH 10 and 0.015 mmol L^{-1} min^{-1} at pH 12 (see series in black on ***Figure 6***).
- In most cases, we observe that in basic medium, the decomposition of GA after its maximum value is faster than in acidic-neutral medium. This effect can explain the higher carbon loss as the pH increases (see ***Figure S9*** for the case of glucose) and is the most pronounced for erythrose conversion over molybdate ions (see ***Figure S8f***).
- Additionally, we observe a special behavior regarding the isomerization of C_6 aldoses by changing the pH. ***Figure S10*** shows the kinetics of fructose and DHA formation for glucose conversion over different tungstate and molybdate precursors at different pH conditions. Tungstates remain nonselective for the isomerization independently of the

precursor and the pH of the reaction medium, while with molybdates we observe an increase in fructose yield and formation rate as the pH increases. With sodium molybdate and AHM at pH 6 and 10 respectively, the yield of fructose is of 10% and 20% at 2 and 5 min of reaction time respectively. The yield of DHA did not exceed 2% in these two experiments.

In the case of tungstates, the hydroxide ions (comparing pH = 7 and pH = 11) only contribute to a minor extent to the cleavage of sugars with a total rate for RAC measured of 0.10 mmol L^{-1} min^{-1} for glucose and 0.12 mmol L^{-1} min^{-1} for mannose (AMT at pH 11). However, this contribution does not explain the increase in GA initial formation rate from pH 4 to pH 7 or 11, thus a pH-driven change of tungstate/sugar speciation must also influence the reaction. On the opposite, the rate of EPI with tungstates decreases with increasing pH. Given the strong pH dependence of tungstate-sugar mixtures, we may infer from that inverse pH dependence in the reaction rates that both reactions are catalyzed by different active species.

Molybdates display a peculiar behavior when pH decreases. The activity towards EPI is very high at pH 4 (0.6 mmol L^{-1} min^{-1} for glucose, 1.4 mmol L^{-1} min^{-1} for mannose) but collapses once the pH increases in the range 0.005-0.030 mmol L^{-1} min^{-1} for pH ≥ 6. The RAC activity remains rather low, with initial rates in the range of 0.020 mmol L^{-1} min^{-1}, and in this case the contribution of hydroxide ions to the RAC cleavage is more significant (around 40-50 %) in the case of molybdates than in the case of tungstates, with initial rates of 0.015 and 0.020 mmol L^{-1} min^{-1} for glucose and mannose, respectively, with AHM at pH 10.

The activity of sugars in epimerization was attributed to dinuclear molybdate species according to Bilik.[20] In our previous contributions, we elucidated the structures of these binuclear species.[29] These species have pH dependent behavior, and they are dominant in acidic-neutral solutions (see ***Figure S11*** and ***S12*** for structures and predominance domains in

the prototypical case of mannose). We found in our previous contribution that these dinuclear species are formed in largest proportions at pH 6 with Mo in the ex-situ study at which a maximum activity in epimerization should be seen, which does not quite match the maximum in epimerization rate determined on ***Figure 6***. However, note that the ex-situ study conducted at higher metals and sugar concentration (2.0 and 1.0 M for the sugar and metal ions, respectively) compared to the catalytic tests that are carried out herein at around 1000-time diluted solution (metal concentration of 1.3 mmol L^{-1}) which impacts significantly the predominance domain of tungstate and molybdate species in aqueous solutions (see ***Figures S13-S20***). By increasing the pH, mononuclear molybdate oxyanions (MoO_4^{2-}) tend to predominate, which might not be able to catalyze the epimerization reaction.

Qualitatively similar behavior is observed with tungstates, with dinuclear complexes with sugars predominant at intermediate pH values and mononuclear species existing at higher pH. Thus, a similar analysis regarding the conversion of sugars with tungstate ions could lead to the conclusion that since epimerization rate slightly decreases with pH, this reaction is catalyzed more efficiently by dinuclear complexes. However, the threshold effect is not pronounced as it is in the case of molybdates, which nuance the conclusion. On the opposite, the rate of RAC increases with pH, thus this reaction should be catalyzed by mononuclear complexes.

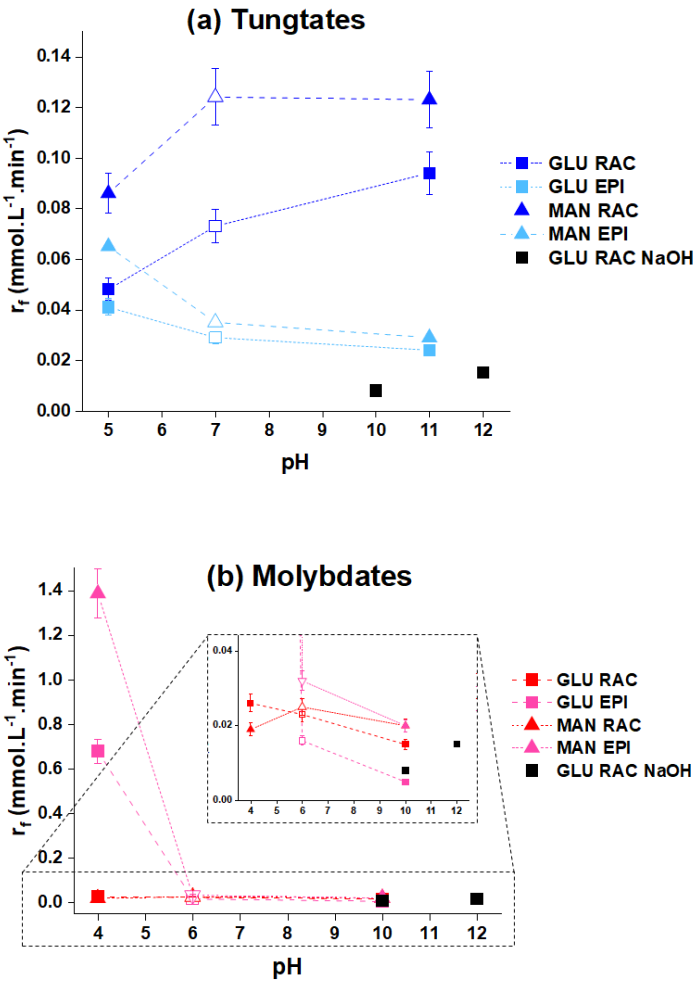

Figure 6. *Initial rates of RAC and epimerization as function of pH for the conversion of C_6 aldoses over (a) tungstate and (b) molybdate catalysts. Full symbols: AMT or AHM precursor; empty symbols: Na_2WO_4 or Na_2MoO_4 precursor. The experiments from which the formation rates were obtained were performed at 150 °C, under 40 bar of N_2, sugar, and metal concentration of respectively 5.0 and 1.3 mmol.L^{-1}. The series in black show the rate of glucose RAC in the absence of catalyst but in the presence of NaOH at the corresponding pH. For molybdates, we show a zoom in the inset.*

Functional groups requirement of the sugars

To get deeper insight into the active species, we investigated on the functional groups' requirements on the sugar that allow the reaction to proceed.

First, we verify that the carbonyl group is mandatory for the cleavage of glucose into C_2 products or epimerization/isomerization products. We carried out the conversion of sorbitol,

which is glucose with a hydrogenated carbonyl group at 150 °C in the presence of 1.3 mmol L^{-1} of AMT at pH 5. After 75 min of reaction time sorbitol was stable without generating any other product, including isomers or fragmentation products (see ***Figure S21***). This confirms that the carbonyl group is mandatory to ensure the reactivity and conversion to fragmentation products. Converting sugar alcohols thus requires a (de)hydrogenation catalytic function in order to generate *in situ* the carbonyl groups that are mandatory for the reactivity of interest herein.[3,4]

Then, to assess the requirements of the various hydroxyl groups of the sugar, we adopted a similar strategy to that conducted by Liu et al.[26] on WO_3 catalysts and carried out the conversion of deoxygenated glucose at different positions, namely 2, 3, 4 and 6. The conversion of 5.0 mmol L^{-1} of 2, 3, 4 and 6-deoxy glucose were conducted over AMT catalyst at tungsten concentration of 1.3 mmol.L^{-1} at 180 °C and pH around 5 since these conditions afforded the highest rates of RAC. ***Figure S22*** shows the different products stemming from the conversion of these modified sugars by retro-aldol condensation, epimerization and isomerization, while the HPLC chromatograms for the conversion of glucose and the different deoxy compounds at 2 min and 8 min of reaction time respectively are shown ***Figure S23***.

Figure 7 shows the evolution with time of the concentration of GA as one of the markers of the RAC reaction, the epimers of the various sugars, and the deoxy-glucose molecules used as reactants themselves. Note that although acetaldehyde should be obtained as a product of the RAC of some of these deoxygenated sugars, or of the deoxy-C4 byproduct, we could not monitor its production, likely because it quickly undergoes side reactions in our reaction conditions. We observe that the formation for GA occurs with all deoxy sugars except 3-deoxy-glucose, which is in line with the scheme on ***Figure S22*** showing the irrelevance of this reaction path for this substrate. We note additionally that in the case of 2-deoxy-glucose, the production of GA is delayed in time, and GA appears as a secondary product, while it appears without

delay for 4- and 6-deoxyglucose with very similar initial rates than with glucose itself. This is also in line with the schemes presented on ***Figure S22*** where a primary RAC with 2-deoxyglucose yields acetaldehyde (that we could not track unambiguously) and erythrose, the RAC of which yields eventually GA as a secondary product. The reactivity of 2-deoxyglucose seems regardless slower than that of other substrates. This set of experiments points toward the conclusion that only the aldehyde and the third hydroxyl groups are a hard requirement to promote the RAC of glucose. This suggests that the other hydroxyl groups (2, 4 and 6) should not be involved in the active species, and thus towards a bidentate complex between O1 and O3. Note that this observation is in sharp contrast with the experiments of Liu et al.,[26] who found that 2-deoxyglucose could not yield ethylene glycol using WO_3 heterogeneous catalysts. This seems to be a specificity of homogeneous tungstate species, and as a consequence, the active species in the case of homogeneous tungstate catalysts must be different from the tridentate active species proposed by Liu et al. on WO_3. Additionally, we note that 4- and 6-deoxyglucose afford lower maximum yields than pristine glucose, which may be partly due to the formation of acetaldehyde as a byproduct, but also, especially in the case of 4-deoxyglucose, to a subtle influence on the reaction rate of the missing hydroxyl group on this substrate, possibly more pronounced on the secondary RAC reaction undergone by the primary product 2-desoxyerythrose.

For the epimerization reaction, of course, 2-deoxy-glucose cannot yield an epimer since this reaction has no relevance in this case. We observe that 6-deoxy-glucose undergoes epimerization at the same rate than glucose, while 3-deoxy-glucose and 4-deoxy-glucose undergo epimerization at respectively lower and higher rates than glucose. These results suggest that the hydroxyl group on carbon atom 3 participate to the active species, though the absence of this group does not prevent the reaction to occur at slower rates. On the opposite, the absence of the hydroxy group on carbon atom 4 increases the reaction rate, which means that not only

it is not mandatory to the formation of the active species, but it rather hinders the reaction. The hydroxy group on C6 is apparently spectator of the reaction, and thus should not participate to the active species. This outcome is rather surprising, as it is not expected under the assumption that similar dinuclear, tetradentate active species are involved for the epimerization catalyzed by tungstates than by molybdates,[20] which should feature the involvement of O1, O2, O3 and O4. Our results rather point towards a tridentate species featuring O1, O2 and O3, though the participation of the latter is not mandatory – simply more favorable. This rather pleads in favor of a mononuclear species in this case, in sharp contrast with the situation with molybdates.

Similar experiments were carried out with AHM as a catalyst (**Figure 8**). **Figure 8a-b** compare the evolution of the concentration of glycolaldehyde and reactant with glucose and 2-deoxy glucose as substrate. In this case the reaction was carried out at 180 °C to maximize the rate of RAC. We observe qualitatively similar rates of formation of glycolaldehyde and consumption of reactant with both substrates, which indicates that the hydroxyl group in position 2 is not involved for the active species leading to the formation of RAC products, which parallels the conclusion made in the case of tungstate catalysts and pleads in favor of a O1-O3 coordination mode, likely with a similar mononuclear species. On the opposite, exposing 3-deoxyglucose to the AHM catalyst (**Figure 8c-d**, at 150 °C) affords the formation of the epimer with a drastically lower rate (0.01 mmol L^{-1} min^{-1}) compared to pristine glucose (0.62 mmol L^{-1} min^{-1}), which shows that the presence of the hydroxyl group on the carbon atom 3 very likely participates to the formation of the most active species. This is in line with earlier proposals and our own results for the involvement of a binuclear tetradentate active species involving O1,O2,O3,O4 (though we only demonstrate the involvement of O1,O2,O3 herein, the existence of such tetradentate species was demonstrated elsewhere[16,28,29]). This does not exclude the presence of other species less active towards epimerization that do not involve

this hydroxyl group and nevertheless contribute to the residual activity observed in this experiment.

Overall, taken together, the results presented in this section tend to indicate that EPI and RAC catalyzed by tungstates could be promoted by two distinct mononuclear complexes, which is consistent with the pH dependency results and the reaction partial order for the catalyst concentration which is lower than unity (between 0.5 and 1). Polynuclear species seem excluded with tungstate catalysts considering these data. In the case of molybdates, RAC seems also catalyzed by mononuclear species involving a O1,O3 coordination mode, while epimerization is consistent with dinuclear species, in agreement with our other results, for instance, the near second order for the catalyst concentration and strong increase in rate at intermediate pH where such species are predominant. Though isostructural species exist with tungstates, they do not seem to be particularly involved in the observed reactions.

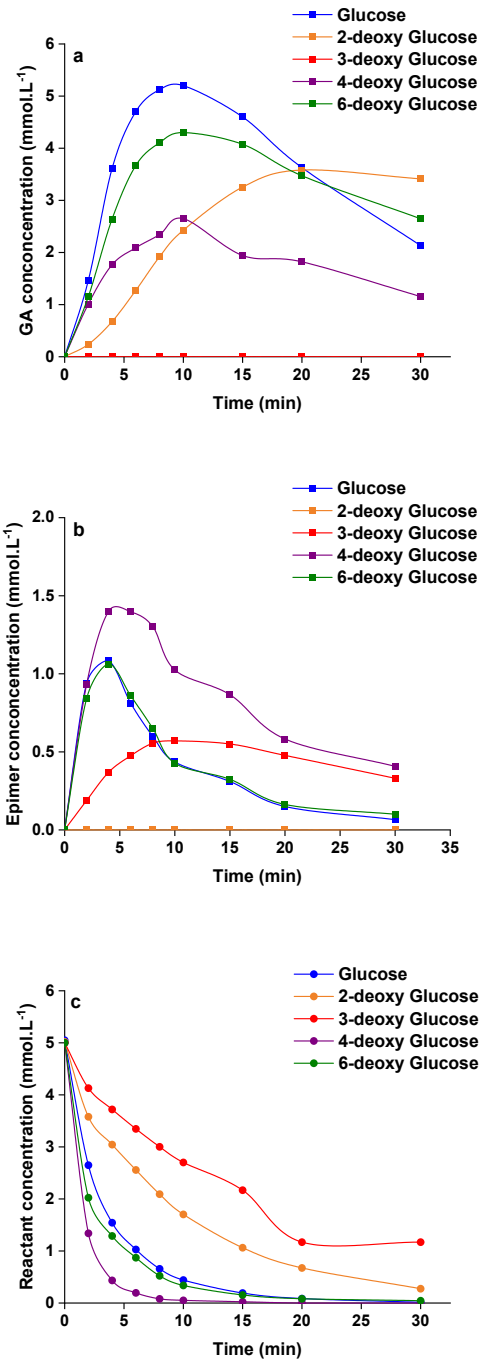

Figure 7. *(a) GA concentration (b) epimer concentration and (c) reactant concentration as a function of reaction time for the conversion of different deoxygenated glucose compounds over AMT catalyst at pH 5, 180 °C, sugars, and tungsten concentration of 5.0 and 1.3 mmol.L^{-1} respectively under 40 bar of N_2.*

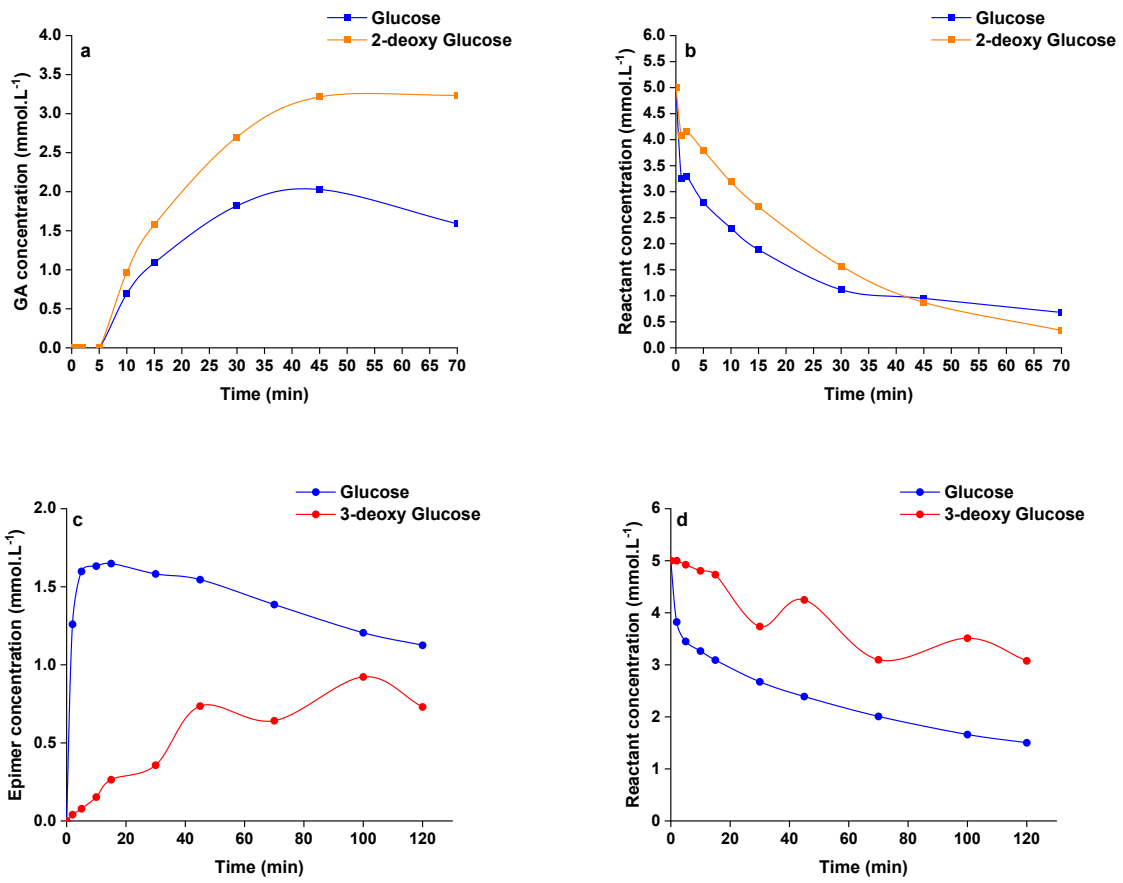

Figure 8. *Conversion of different deoxygenated glucose compounds over AHM catalyst at pH 5, sugars and molybdenum concentrations of 5.0 and 1.3 mmol.L^{-1} respectively under 40 bar of N_2. (a) GA concentration and (b) reactant concentration for glucose and 2-deoxy-glucose conversion at 180 °C; (c) epimer and (d) reactant concentrations for glucose and 2-deoxy-glucose conversion at 150 °C.*

Effect of reducing atmosphere

So far, the reactivity of tungstate and molybdate towards carbohydrates was evaluated under inert atmosphere (N_2). However, in several applications, for instance, the production of ethylene glycol, the catalysts are to be used under hydrogen atmosphere, hence with a potential reduction of the W or Mo. In fact, Zhang and coworkers assigned the potential active species to partially reduced tungsten species, called tungsten bronzes (soluble H_xWO_3).[10,22] **Figure 9** shows the kinetics of GA formation over AMT and AHM catalysts under inert and reducing atmospheres.

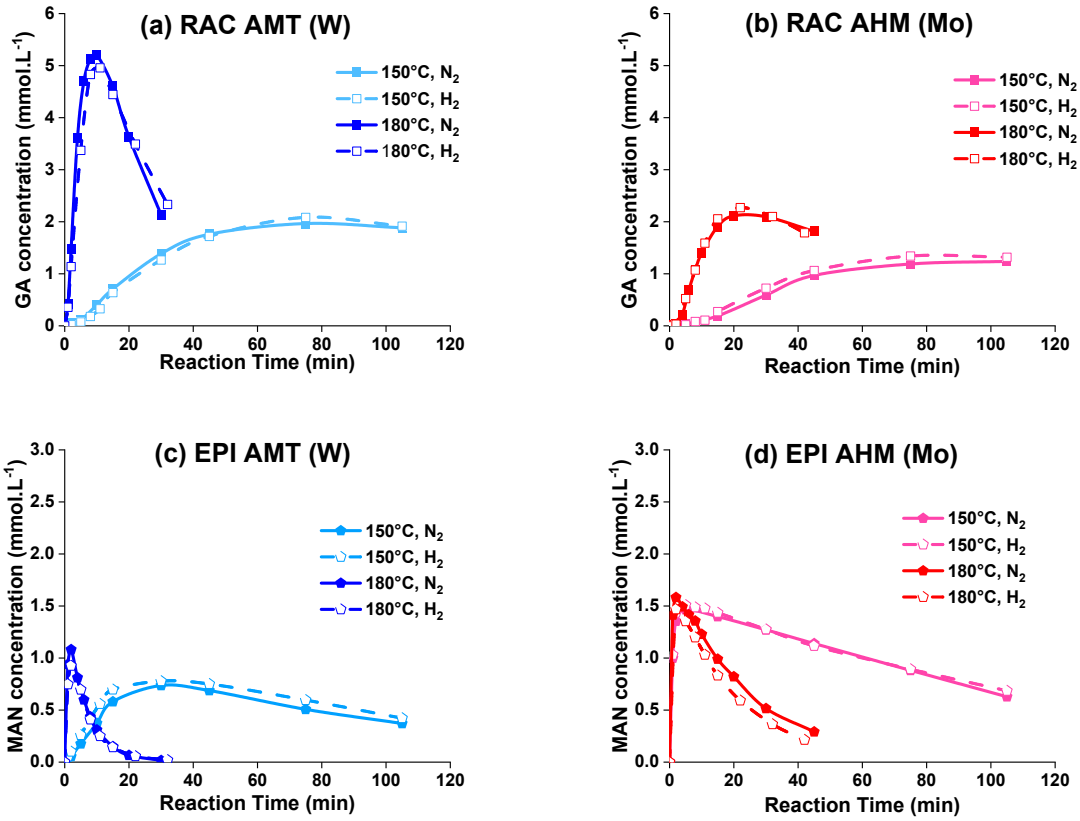

Figure 9. *Kinetics of GA (a,b) and mannose (c,d) formation for glucose conversion over (a,c) AMT (pH 5) and (b,d) AHM (pH 4) catalysts at different temperatures, metals, and glucose concentrations of 1.3 and 5.0 mmol.L^{-1} respectively and 40 bar of N_2/H_2.*

We verify here that performing the reaction under N_2 or H_2 atmosphere (40 bar) does not change the results to a significant extent. This shows that i) the results are not dependent on the atmosphere, thus the conclusions drawn herein should still be valid under H_2 atmosphere; ii) the hypothesis of a partially reduced active species is very unlikely for both RAC and epimerization, as in the opposite case switching to a reducing atmosphere should have increased the rate of one or the other. This is true at the two temperatures investigated herein (150 and 180 °C).

Note that in our study no hydrogenation catalyst was added in the medium. We nevertheless find apparent activation energy for the RAC reaction catalyzed by AMT in the presence of N_2 very close to that obtained by Zhang et al. in the presence of both AMT and a Ru/C hydrogenation catalyst (160 kJ mol^{-1} by Zhang et al. *versus* 157 kJ mol^{-1} in the present work).[40]

This points to similar mechanisms and reactivity despite the presence of H_2 and hydrogenation catalyst.

3.3. In situ XANES

An in-situ follow up of the reaction was carried out using XANES characterization to gain additional insight into the structure and oxidation state of the metal during the reaction. ***Figures S24*** and ***S25*** illustrate respectively the XANES W L_3-edge and Mo K-edge spectra of tungstate and molybdate precursors that allow distinguishing between the features of oligomeric octahedral (AMT and AHM) and monomeric tetrahedral (Na_2WO_4 and Na_2MoO_4) tungstate and molybdate species. Note that these experiments were carried out under He atmosphere instead of N_2, as we did for the kinetic experiments. This is not expected to affect the results, since even using a potentially reactive gas did not modify the outcome of the reaction to a measurable extent (H_2, see **Figure 9**).

Conversion of sugars over AMT catalyst

The follow up of the conversion of glucose and mannose over AMT at different temperatures, metals concentrations and pH was carried out by *in-situ* experiments. The XANES spectra for glucose conversion, at different reaction times and under different reaction conditions at a reaction time of 20 min are shown on ***Figure 10a-b***, and the complete follow-up spectra for glucose, mannose and erythrose at the reaction conditions under study are shown on ***Figure S26-S28***.

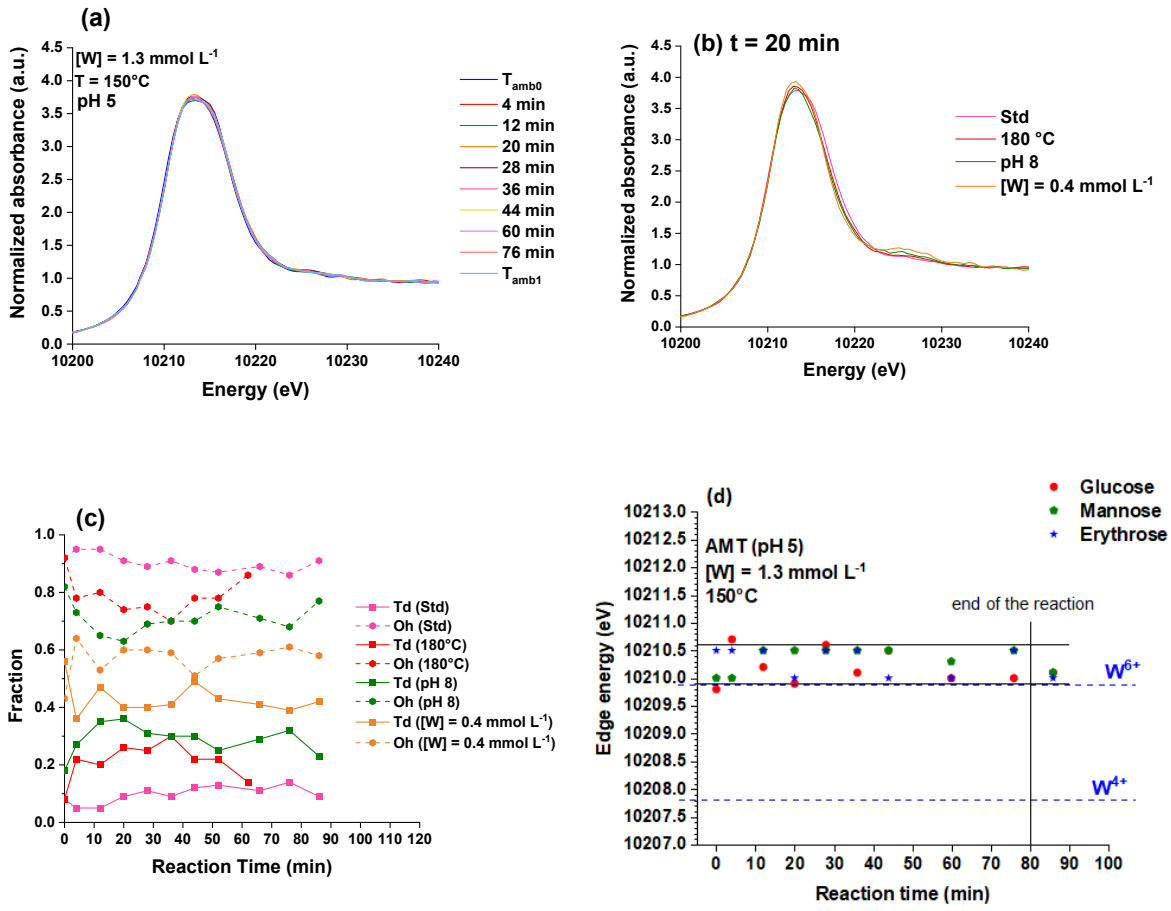

Figure 10. *(a) W L_3-edge XANES spectra for the follow up of glucose conversion over AMT catalyst under Standard (Std) reaction conditions, (b) W L_3-edge XANES spectra conversion of glucose over AMT catalyst at different reaction conditions at 20 min of reaction time, (c) Variation of tetrahedral(Td) and octahedral(Oh) species through the reaction time for the conversion of glucose with AMT catalysts at different reaction conditions, (d) Evolution of the edge energy of tungsten through the reaction time for glucose, mannose, and erythrose conversion under Standard conditions. The black solid lines show the highest and the lowest edge energy detected for +VI tungstate precursors measured in our experiments. The blue dashed lines represent the edge energy of W^{4+} (measurement made in the present work from WO_2).*
Standard (Std) experiment performed at sugar and tungsten concentration of 5.0 and 1.32 mmol L^{-1} respectively, 150°C under 40 bar of He. The parameters indicated in the legend represent the difference from the Std experiment.

Similar spectra are recorded for glucose conversion during the reaction over AMT regardless the change pH and tungsten concentration. In the case of mannose and erythrose, the spectra are very similar as well regardless of the composition and reaction temperature. This indicates little structural evolution of the metal centers in the course of the reaction, though slight variations exist depending on the initial conditions which might be related to the co-

existence of variable proportions of octahedral and tetrahedral species. To obtain more quantitative assessment of the speciation, we decomposed the XANES spectra by linear combination fitting using the spectra of the reference compounds Na_2WO_4 (Td) and AMT (Oh) (see example on ***Figure S29a***). The corresponding aqueous solutions at [W] = 0.1 M, respectively of pH 10 and 4 indeed feature exclusively tetrahedral and octahedral species, respectively (see Figure S13), thus constitute fair reference for each geometry. Decomposition of the signal into octahedral and tetrahedral contributions from the reference spectra can be found on ***Figure 10c*** in the case of glucose (***Figure S30*** for mannose), which confirms little evolution during the reaction despite the significant evolution of the composition of the reaction medium (consumption of sugar, appearance of products). Octahedrally-shaped is dominant (fraction higher than 60 % in most cases) but coexistence of tetrahedral species is always observed.

We measured the evolution of the edge energy detected at the different experiments through the reaction time and compared them to the edge energy of free AMT featuring +VI oxidation states to evaluate if a reduction of the metal has occurred due to the presence a reducing sugar as glucose, mannose and erythrose, or any product of the reaction. The results are shown in ***Figure 10d.*** No significant variation of the edge energy can be observed, thus no clear evidence for a reduction of tungsten appears since the distribution of the points is homogenous between the highest and the lowest values characterizing +VI oxidation state. This remains true for the three sugars and for each conversion condition under investigation (see ***Figure S31***).

Conversion of sugars over AHM catalyst

Figure 11a and ***b*** show respectively the spectra recorded by *in-situ* XANES measurements for the conversion of glucose under Standard conditions at different reaction times, and at 20

min of reaction time under different reaction conditions with AHM catalyst (additional spectra including erythrose and mannose as substrate are available on ***Figures S32-S34***).

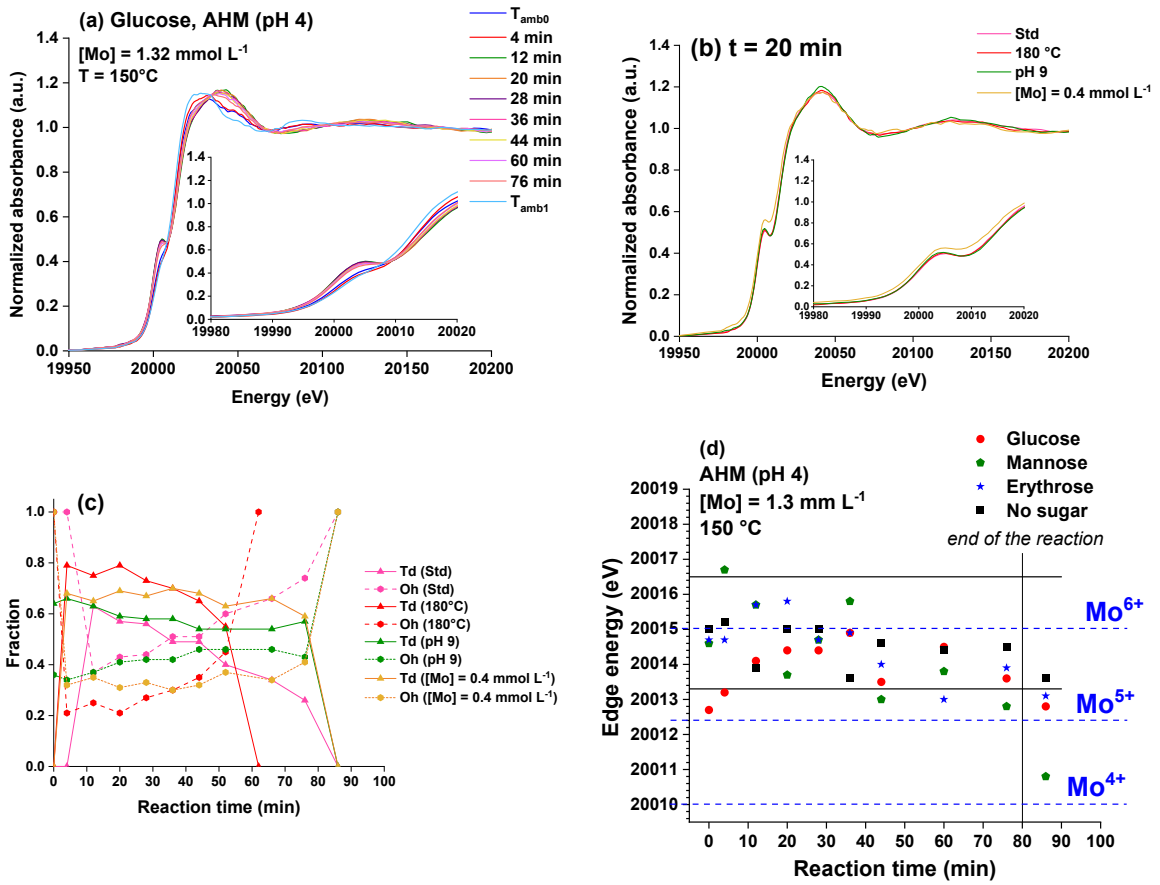

Figure 11. *(a) Mo K-edge XANES spectra for the follow up of glucose conversion over AHM catalyst under Standard (Std) reaction conditions, (b) Mo K-edge XANES spectra conversion of glucose over AHM catalyst at different reaction conditions at 20 min of reaction time, (c) Variation of Td and Oh species through the reaction time for the conversion of glucose and mannose with AHM catalysts at different reaction conditions; (d) Evolution of the edge energy of molybdenum through the reaction time for glucose, mannose, and erythrose conversion at Standard conditions. The black solid lines show the highest and the lowest edge energy detected for 6+ molybdenum precursors measured in our experiments. The blue dashed lines represent the edge energy of* Mo^{6+}, Mo^{5+}, *and* Mo^{4+} *obtained from the literature.*[41,42]
Standard (Std) experiment performed at sugar and tungsten concentration of 5.0 and 1.32 mmol L^{-1} *respectively, 150 °C under 40 bar of He. The parameters indicated in the legend represent the difference from the Std experiment.*

In the course of the reaction, the intensity of the pre-edge increases, while the white line shape changes in intensity and position for the conversion of all sugars independently of the reaction conditions. This evolution is characterized by the presence of four isosbestic points at 20032, 20067, 20103 and 20147 eV, which is characteristic of the interconversion between two

species.[43] The change is faster at 180 °C rather than 150 °C. To check whether it is an effect of the temperature or the presence of the sugar, a solution of AHM in the absence of sugar was heated at 150°C. ***Figure S34*** shows the corresponding *in situ* Mo K-edge spectra, on which a similar effect is observed, with the same isosbestic points detected than for glucose and mannose-AHM solutions (20032, 20067, 20103 and 20147 eV), thus this effect is partly related to the evolution of the speciation of molybdate ions with temperature. To obtain more quantitative assessment of the speciation, we decomposed the XANES spectra by linear combination fitting using the spectra of the reference compounds Na_2MoO_4 (Td) and AHM (Oh) – see example on ***Figure S29b***. The corresponding aqueous solutions at [Mo] = 0.1 M, respectively of pH 10 and 4 indeed feature exclusively tetrahedral and octahedral species, respectively (see Figure S17), thus constitute fair reference for each geometry. The results are shown on ***Figure 11c*** for glucose and ***Figure S36*** for mannose, and demonstrate that the composition during reaction varies more significantly than in the case of tungstates, with the fraction of octahedral species increasing with reaction time in most cases. Cooling down to ambient temperature after reaction restores the initial octahedral coordination in all cases.

The evolution of the oxidation state of Mo through the reaction at the different conditions is shown on ***Figure 11d*** for the three sugars under standard conditions. The evolution of the oxidation states differs slightly according to the reaction conditions. At pH 4 and molybdenum concentration of 1.3 mmol L^{-1}, this evolution is characterized by a slight shift towards lower energies (20010.8 eV and 20011.6 eV are the lowest edge-energies detected at 150 and 180 °C respectively) especially after the end of the reaction (***Figure 11d*** and ***Figure S37a-b*****).** All the energy values were distributed between the reference values attributed to +VI and +V oxidation states. For the experiments at pH 10 and lower metal concentration the edge energies are more shifted to high values, consistent with +VI oxidation state (***Figure S37c-d)***. A possible partial reduction might then occur at specific conditions of pH and metal concentration, but this would

be a phenomenon that occurs slowly during the reaction. Thus, at short reaction times, molybdenum probably exists essentially in +VI oxidation state. Note that this evolution also occurs to some extent in the absence of sugar, thus, akin to the structural evolution noted, this might be principally due to the temperature. Since we have shown that the activity of molybdenum in RAC is independent of the pH, we may infer that the reduction is either too minor to significantly influence the reaction or has little influence on the reactivity of molybdenum.

4. Conclusion

The present contribution presents a comparative study of tungstate- and molybdate-based homogeneous catalysis of the conversion of biomass-based sugars, more specifically aldoses (glucose, mannose and erythrose). We address the questions of the potential active sites for epimerization and retro-aldol condensation, which are the major reaction paths observed in these conditions, and of the oxidation state of the metal, via a combination of kinetic experiments and *in situ* XANES characterization. We gather a series of new insights on the reaction mechanisms.

In particular, we show that for tungsten-based homogeneous catalysts, the active species for EPI and RAC are very likely a bidentate mononuclear species involving the O1 and O2 (EPI) and O1 and O3 groups (RAC). For molybdate-based catalysts, two different active species may also be invoked: a mononuclear O1,O3 species for RAC, possibly isostructural to that in the case of tungstate, and another binuclear species, at least tridentate O1,O2,O3 – and likely tetradentate O1,O2,O3,O4. **Figure 12** proposes a summary of potential active species according to our results.

We further show that both main reactions (RAC and EPI) occur in the presence of +VI oxidation state metals. While the existence of reduced species in the case of the presence of a hydrogenating catalytic function is possible – we did not examine this case here – their presence does not seem to be a requirement, and we obtain similar activation energy for the RAC using AMT under N_2 than previously obtained data using AMT, Ru/C under H_2 atmosphere,[40] which pleads in favor of similar active species and thus oxidation state.

Bringing new understanding, the current conclusions pave the way to the optimal control of the selectivity and of the activity of both metals as a function of operating conditions.

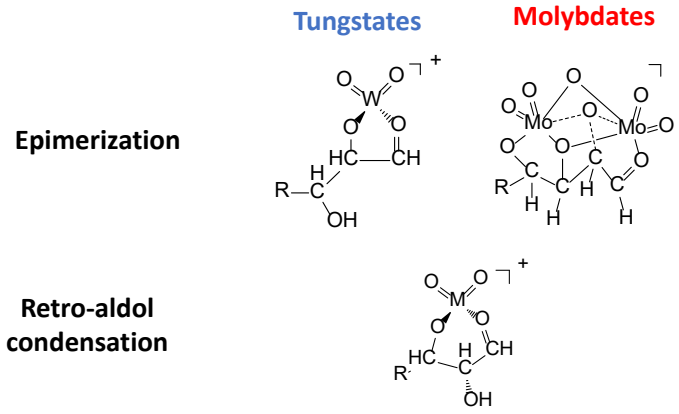

Figure 12. *Proposal of active species for the two main reactions with tungstates or molybdates. R stands for the remainder of the sugar molecule*

ASSOCIATED CONTENT

AUTHOR INFORMATION

Corresponding Author

Kim Larmier – IFP Energies nouvelles, Solaize 69360, France ; orcid.org/0000-0002-5199-1516 ; Email : kim.larmier@ifpen.fr

Notes

The authors declare no competing financial interests.

SUPPORTING INFORMATION

Additional kinetic experiment data, simulations of aqueous-phase speciation of W- and Mo-species, photographs of experimental XANES setup, additional XANES data. The following files are available free of charge.

ACKNOWLEDGMENT

The authors acknowledge the European Synchrotron Radiation Facility (ESRF) (Grenoble, France) and the CRG-FAME BM30 beamline (French Absorption spectroscopy beamline in Material and Environmental science) staff for the XAS experiments.

References

(1) Corma, A.; Iborra, S.; Velty, A. Chemical routes for the transformation of biomass into chemicals. *Chemical Reviews* **2007**, *107*, 2411–2502.

(2) Putro, J. N.; Soetaredjo, F. E.; Lin, S.-Y.; Ju, Y.-H.; Ismadji, S. Pretreatment and conversion of lignocellulose biomass into valuable chemicals. *RSC Adv.* **2016**, *6*, 46834–46852.

(3) Rivière, M.; Perret, N.; Cabiac, A.; Delcroix, D.; Pinel, C.; Besson, M. Xylitol Hydrogenolysis over Ruthenium-Based Catalysts:Effect of Alkaline Promoters and Basic Oxide-Modified Catalysts. *ChemCatChem* **2017**, *9* (12), 2145–2159. DOI: 10.1002/cctc.201700034.

(4) Liu, H.; Huang, Z.; Xia, C.; Jia, Y.; Chen, J.; Liu, H. Selective Hydrogenolysis of Xylitol to Ethylene Glycol and Propylene Glycol over Silica Dispersed Copper Catalysts Prepared by

a Precipitation-Gel Method. *ChemCatChem* **2014**, *6* (10), 2918–2928. DOI: 10.1002/cctc.201402141.

(5) Wang, X.; Wu, F.; Yao, S.; Jiang, Y.; Guan, J.; Mu, X. Ni–Cu/ZnO-catalyzed Hydrogenolysis of Cellulose for the Production of 1,2-Alkanediols in Hot Compressed Water. *Chem. Lett.* **2012**, *41* (5), 476–478. DOI: 10.1246/cl.2012.476.

(6) Gallezot, P.; Nicolaus, N.; Flèche, G.; Fuertes, P.; Perrard, A. Glucose Hydrogenation on Ruthenium Catalysts in a Trickle-Bed Reactor. *J. Catal.* **1998**, *180*, 51–55.

(7) Delidovich, I.; Palkovits, R. Catalytic Isomerization of Biomass-Derived Aldoses:A Review. *ChemSusChem* **2016**, *9* (6), 547–561. DOI: 10.1002/cssc.201501577.

(8) Liu, C.; Zhang, C.; Hao, S.; Sun, S.; Liu, K.; Xu, J.; Zhu, Y.; Li, Y. WO modified Cu/Al2O3 as a high-performance catalyst for the hydrogenolysis of glucose to 1,2-propanediol. *Catalysis Today* **2016**, *261*, 116–127. DOI: 10.1016/j.cattod.2015.06.030.

(9) Liu, Y.; Luo, C.; Liu, H. Tungsten trioxide promoted selective conversion of cellulose into propylene glycol and ethylene glycol on a ruthenium catalyst. *Angew. Chem. Int. Ed.* **2012**, *51* (13), 3249–3253. DOI: 10.1002/anie.201200351. Published Online: Feb. 24, 2012.

(10) Tai, Z.; Zhang, J.; Wang, A.; Pang, J.; Zheng, M.; Zhang, T. Catalytic conversion of cellulose to ethylene glycol over a low-cost binary catalyst of Raney Ni and tungstic acid. *ChemSusChem* **2013**, *6* (4), 652–658. DOI: 10.1002/cssc.201200842.

(11) Wang, A.; Zhang, T. One-pot conversion of cellulose to ethylene glycol with multifunctional tungsten-based catalysts. *Acc. Chem. Res.* **2013**, *46* (7), 1377–1386. DOI: 10.1021/ar3002156.

(12) Zhao, G.; Zheng, M.; Zhang, J.; Wang, A.; Zhang, T. Catalytic Conversion of Concentrated Glucose to Ethylene Glycol with Semicontinuous Reaction System. *Ind. Eng. Chem. Res.* **2013**, *52* (28), 9566–9572. DOI: 10.1021/ie400989a.

(13) Petrus, L.; Petrusova, M.; Hricoviniova, Z. *The Bílik Reaction*; Topics in Current Chemistry, Vol. 215; Springer, 2001.

(14) Bilik, V.; Knezek, I. Reactions of Saccharides Catalyzed by Molybdate Ions XLV. Utilization of Molybdic and Peroxomolybdic Acids for Preparation of Aldoses. *Chemistry Papers* **1992**, *46*, 193–195.

(15) Bilik, V.; Petrus, L.; Farkas, V. Reactions of Saccharides Catalyzed by Molybdate ions XLIL. Epimerization and the Molybdate Complexes of the Aldoses. *Chem. Zvesti* **1975**, *29*, 690–693.

(16) Bilik, V.; Matulova, M. Reactions of saccharides catalyzed by molybdate ions XLII. Epimerization and the molybdate complexes of aldoses. *Chem. Papers* **1990**, *44*, 257–265.

(17) Oyerinde, O. F.; Weeks, C. L.; Anbar, A. D.; Spiro, T. G. Solution structure of molybdic acid from Raman spectroscopy and DFT analysis. *Inorg. Chim. Acta* **2008**, *361* (4), 1000–1007. DOI: 10.1016/j.ica.2007.06.025.

(18) Hur, H.; Reeder, R. J. Tungstate sorption mechanisms on boehmite: Systematic uptake studies and X-ray absorption spectroscopy analysis. *J. Colloid. Interface Sci.* **2016**, *461*, 249–260. DOI: 10.1016/j.jcis.2015.09.011. Published Online: Sep. 5, 2015.

(19) Hayes, M. L.; Pennings, N. J.; Serianni, A. S.; Barker, R. Epimerization of aldoses by molybdate involving a novel rearrangement of the carbon skeleton. *J. Am. Chem. Soc.* **1982**, *104*, 6764–6769.

(20) Bilik, V.; Matulova, M. Reactions of saccharides catalyzed by molybdate ions XLII. Epimerization and the molybdate complexes of aldoses. *Chemistry Papers* **1990**, *44*, 257–265.

(21) Chethana, B. K.; Lee, D.; Mushrif, S. H. First principles investigation into the metal catalysed 1,2 carbon shift reaction for the epimerization of sugars. *J. Mol. Cat. A: Chem.* **2015**, *410*, 66–73. DOI: 10.1016/j.molcata.2015.09.004.

(22) Tai, Z.; Zhang, J.; Wang, A.; Zheng, M.; Zhang, T. Temperature-controlled phase-transfer catalysis for ethylene glycol production from cellulose. *Chem. Comm.* **2012**, *48* (56), 7052–7054. DOI: 10.1039/c2cc32305b.

(23) Chu, D.; Zhao, C. Reduced oxygen-deficient CuWO4 with Ni catalyzed selective hydrogenolysis of cellulose to ethylene glycol. *Catal. Tod.* **2020**, *351*, 125–132. DOI: 10.1016/j.cattod.2018.10.006.

(24) Qiao, Y.; Xia, G.-J.; Cao, W.; Zeng, K.-H.; Guo, Q.-L.; Yang, X.-F.; Wang, A.-Q.; Wang, Y.-G. Breaking the C C bond of glucose on tungsten oxide-based catalysts in aqueous phase. *J. Catal.* **2023**, *427*, 115114. DOI: 10.1016/j.jcat.2023.115114.

(25) Zhang, J.; Hou, B.; Wang, A.; Li, Z.; Wang, H.; Zhang, T. Kinetic study of retro-aldol condensation of glucose to glycolaldehyde with ammonium metatungstate as the catalyst. *AIChE J.* **2014**, *60* (11), 3804–3813. DOI: 10.1002/aic.14554.

(26) Liu, Y.; Zhang, W.; Hao, C.; Wang, S.; Liu, H. Unveiling the mechanism for selective cleavage of C-C bonds in sugar reactions on tungsten trioxide–based catalysts. *Proc. Natl. Acad. Sci. U.S.A.* **2022**, *119* (34). DOI: 10.1073/pnas.2206399119.

(27) Zhang, J.; Hou, B.; Wang, A.; Li, Z.; Wang, H.; Zhang, T. Kinetic study of the competitive hydrogenation of glycolaldehyde and glucose on Ru/C with or without AMT. *AIChE J.* **2015**, *61* (1), 224–238. DOI: 10.1002/aic.14639.

(28) El Mohammad, S.; Proux, O.; Aguilar Tapia, A.; Hazemann, J. L.; Legens, C.; Chizallet, C.; Larmier, K. Elucidation of Metal-Sugar Complexes: When Tungstate Combines with D-Mannose. *Inorg. Chem.* **2023**, *62*, 7545–7556.

(29) El Mohammad, S.; Develle, S.; Proux, O.; Aguilar Tapia, A.; Hazemann, J. L.; Legens, C.; Chizallet, C.; Larmier, K. Deciphering the Structure of Tungstate and Molybdate Complexes with Glucose, Mannose, and Erythrose. *Inorg. Chem.* **2024**, *63*, 3129–3136.

(30) Verchère, J.-F.; Sauvage, J.-P.; Rapaumbya, G.-R. Comparative study of various polyols as complexing agents for the acidimetric titration of tungstate. *Analyst* **1990**, *115*, 637–640.

(31) Chapelle, S.; Verchère, J.-F. Tungsten-183 NMR studies of tungstate complexes of carbohydrates. 1. Characterization of two structural types in the alditol series. Evidence that the tungstate and molybdate threo complexes are not homologous. *Inorg. Chem.* **1992**, *31*, 648–652.

(32) Chapelle, S.; Verchère, J.-F. A carbon-13 NMR study of the tungstate and molybdate complexes of perseitol, galacticol and mannitol. *Carbohydr. Res.* **1991**, *211*, 279–286.

(33) Chapelle, S.; Sauvage, J.-P.; Verchère, J.-F. 183W NMR Studies of Tungstate Complexes of Carbohydrates. 2. Competitive Formation of erythro and threo Complexes of Alditols. Characterization of a Novel Bis-Dinuclear Complex Formed with Perseitol. *Inorg. Chem.* **1994**, *33*, 1966–1971.

(34) Proux, O.; Nassif, V.; Prat, A.; Ulrich, O.; Lahera, E.; Biquard, X.; Menthonnex, J. J.; Hazemann, J. L. Feedback system of a liquid-nitrogen-cooled double-crystal monochromator: design and performances. *J. Synchrotron Radiat.* **2006**, *13* (Pt 1), 59–68. DOI: 10.1107/S0909049505037441. Published Online: Dec. 22, 2005.

(35) Proux, O.; Biquard, X.; Lahera, E.; Menthonnex, J.-J.; Prat, A.; Ulrich, O.; Soldo, Y.; Trévisson, P.; Kapoujyan, G.; Perroux, G.; Taunier, P.; Grand, D.; Jeantet, P.; Deleglise, M.; Roux, J.-P.; Hazemann, J. L. FAME: a New Beamline for X-Ray Absorption Investigations of Very-Diluted Systems of Environmental, Material and Biological Interests. *Physica Scripta* **2005**, *T115*, 970–973.

(36) Testemale, D.; Argoud, R.; Geaymond, O.; Hazemann, J. L. High Pressure/High Temperature Cell for X-Ray Absorbtion and Scattering Techniques. *Rev. Sci. Inst.* **2005**, *76*, 1–5.

(37) Ravel, B.; Newville, M. ATHENA, ARTEMIS, HEPHAESTUS: data analysis for X-ray absorption spectroscopy using IFEFFIT. *J. Synchrotron Radiat.* **2005**, *12* (Pt 4), 537–541. DOI: 10.1107/S0909049505012719. Published Online: Jun. 15, 2005.

(38) Angyal, S. J. A Short Note on the Epimerization of Aldoses. *Carbohydr. Res.* **1997**, *300*, 279–281.

(39) van Zandvoort, I.; Wang, Y.; Rasrendra, C. B.; van Eck, E. R. H.; Bruijnincx, P. C. A.; Heeres, H. J.; Weckhuysen, B. M. Formation, molecular structure, and morphology of humins in biomass conversion:Influence of feedstock and processing conditions. *ChemSusChem* **2013**, *6* (9), 1745–1758. DOI: 10.1002/cssc.201300332.

(40) Zhao, G.; Zheng, M.; Sun, R.; Tai, Z.; Pang, J.; Wang, A.; Wang, X.; Zhang, T. Ethylene glycol production from glucose over W-Ru catalysts: Maximizing yield by kinetic modeling and simulation. *AIChE Journal* **2017**, *63* (6), 2072–2080. DOI: 10.1002/aic.15589.

(41) Farges, F.; Siewert, R.; Brown, G. E.; Guesdon, A.; Morin, G. Structural Environments Around Molybdenum in Silicate Glasses and Melts. I. Influence of Composition and Oxygen Fugacity on The Local Structure Of Molybdenum. *The Canadian Mineralogist* **2006**, *44*, 731–753. DOI: 10.2113/gscanmin.44.3.731.

(42) Kopachevska, N. S.; Melnyk, A. K.; Bacherikova, I. V.; Zazhigalov, V. A.; Wieczorek-Ciurowa, K. Determination of Molybdenum Oxidation State on The Mechanochemically Treated MoO3. *Him. Fiz. Tehnol. Poverhni* **2015**, *6* (4), 474–480. DOI: 10.15407/hftp06.04.474.

(43) Vardevanyan, P. O.; Élbakyan, V. L.; Shahinyan, M. A.; Minasyants, M. V.; Parsadanyan, M. A.; Sahakyan, N. S. Determination of the Isosbestic Point in the Absorption Spectra of DNA–Ethidium Bromide Complexes. *J. Appl. Spectrosc.* **2015**, *81*, 1060–1063. DOI: 10.1007/s10812-015-0051-x.